Passivation effects of phosphorus on 4H-SiC (0001) Si dangling bonds: A first-principles study*

Wenbo Li(李文波)[1,†], Ling Li(李玲)[2,†], Fangfang Wang(王方方)[2], Liu Zheng(郑柳)[2], Jinghua Xia(夏经华)[2], Fuwen Qin(秦福文)[3], Xiaolin Wang(王晓琳)[1], Yongping Li(李永平)[2], Rui Liu(刘瑞)[2], Dejun Wang(王德君)[1], Yan Pan(潘艳)[2,‡], and Fei Yang(杨霏)[2,4,§]

[1] *School of Electronic Science and Technology, Faculty of Electronic Information and Electrical Engineering, Dalian University of Technology, Dalian* 116024, *China*

[2] *Global Energy Interconnection Research Institute, Beijing* 102211, *China*

[3] *State Key Laboratory of Materials Modification by Laser, Ion and Electron Beams (Ministry of Education), Dalian University of Technology, Dalian* 116024, *China*

[4] *State key Laboratory of Advanced Power Transmission Technology, Beijing* 102211, *China*

(Received 11 November 2016; revised manuscript received 19 December 2016; published online 18 January 2017)

The effect of phosphorus passivation on 4H-SiC(0001) silicon (Si) dangling bonds is investigated using *ab initio* atomistic thermodynamic calculations. Phosphorus passivation commences with chemisorption of phosphorus atoms at high-symmetry coordinated sites. To determine the most stable structure during the passivation process of phosphorus, a surface phase diagram of phosphorus adsorption on SiC (0001) surface is constructed over a coverage range of 1/9–1 monolayer (ML). The calculated results indicate that the 1/3 ML configuration is most energetically favorable in a reasonable environment. At this coverage, the total electron density of states demonstrates that phosphorus may effectively reduce the interface state density near the conduction band by removing 4H-SiC (0001) Si dangling bonds. It provides an atomic level insight into how phosphorus is able to reduce the near interface traps.

Keywords: phosphorus passivation, silicon carbide, near interface traps, surface phase diagram

PACS: 71.20.Nr, 73.20.At, 68.35.Dv **DOI:** 10.1088/1674-1056/26/3/037104

1. Introduction

Silicon carbide (SiC) has a wide application in extremely harsh environments. Besides, it is also a promising wide-band-gap semiconductor material for fabrication of high-temperature, high-frequency, and high-power metal–oxide–semiconductor (MOS) devices due to its excellent physical properties as well as native oxide (SiO_2).[1–4] Among the commercially available SiC polytypes, 4H-SiC is most attractive for high-power electronic devices such as MOS field effect transistors (MOSFETs) owing to its higher bulk electron mobility and smaller anisotropy.[5,6] However, the high density of interface traps (Dit) near the conduction band edge at the SiO_2/SiC (0001) interface gives rise to the low channel mobility of 4H-SiC MOSFETs.[7–10] It is therefore important to passivate the interface to improve the channel mobility of SiC MOSFETs.

A large number of process methods have been tried to reduce the defect density to an acceptable level. It has been demonstrated experimentally that the interface state densities can be significantly reduced by annealing SiO_2/SiC interfaces with nitrogen (N).[11–21] Unfortunately, the obtained Dit ($\sim 2\times10^{11}$ cm^{-2}·eV^{-1}) after nitridation treatment is still too high for SiC MOS capacitors.[13] It is necessary to explore new passivation processes to achieve higher mobility for 4H-SiC MOSFETs. Okamoto *et al.* recently attempted to reduce the Dit by post-oxidation annealing in phosphoryl chloride ($POCl_3$).[22–25] Their results showed that the Dit was effectively reduced by phosphorus (P) atoms and the peak field-effect mobility of 4H-SiC MOSFETs could be increased to 89 cm^2/V·s. Their subsequent studies suggested that the positive effects of P atoms might be attributed to the passivation of NITs, in particular, the elimination of Si–Si bonds.[26] However, atomic scale understanding of phosphorus at the interface has remained unclear.

Experiments have reported many kinds of defects exist at the SiO_2/SiC interface. The dangling bond defect, as a simple interface defect, is also found at the SiO_2/SiC interface,[27] similar to the SiO_2/Si interface.[28] Pennington and Ashman recently used density functional theory (DFT) calculations to investigate nitrogen passivation of 4H-SiC (0001) Si-face dangling bonds.[19–21] That work showed that the Si dangling bonds may create states below the conduction band edge and the dangling bond defect states may be removed by nitrogen. However, little is still known about the effects of phosphorus

*Project supported by the National High Technology Research and Development Program of China (Grant No. 2014AA052401), the National Natural Science Foundation of China (Grant No. 61474013), and the National Grid Science & Technology Project, China (Grant No. 5455DW150006).

†Wenbo Li and Ling Li contributed equally to this work.

‡Corresponding author. E-mail: panyan@geiri.sgcc.com.cn

§Corresponding author. E-mail: yangsenji@163.com

© 2017 Chinese Physical Society and IOP Publishing Ltd

passivation on the dangling bonds. In this work, we study the effect of phosphorus passivation 4H-SiC (0001) Si dangling bonds by using the first-principles approach, in order to better understand the removal mechanism of the defect states.

2. Computation methods

DFT calculation is performed using Cambridge serial total energy package (CASTEP) code. The generalized gradient approximation (GGA) function proposed by Perdew and Wang (PW91)[29] and a plane-wave cutoff of 300 eV are employed after a full convergence test. The Vanderbilt ultrasoft pseudopotentials[30] are used to describe the ion–electron interaction. The equilibrium atomic positions are determined when the maximum Hellmann–Feynman force and the change of the total energy are below 0.03 eV/Å and 0.01 meV, respectively. The optimized lattice constants are $a = 3.078$ Å and $c = 10.046$ Å using a $9 \times 9 \times 2$ Monkhorst–Pack grid, agreeing well with the experimental values ($a = 3.073$ Å and $c = 10.053$ Å).

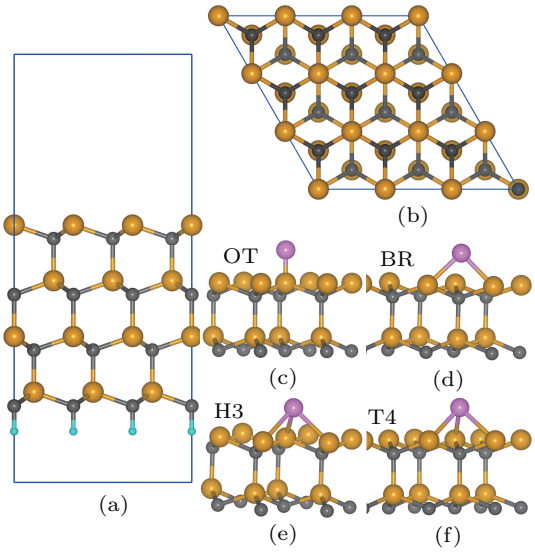


Fig. 1. (color online) (a) Side and (b) top views of 4H-SiC (0001) surface and (c), (d) four adsorption sites on this surface. The on-top site (OT) is located on the top of a surface Si atom, the bridge site (BR) is a two-fold coordinated site between two surface Si atoms, the three-fold hollow site (H3) is above a carbon of the third bilayer, and the four-fold hollow site (T4) is above a carbon of the first bilayer. The orange, grey, magenta, and cyan spheres denote silicon, carbon, phosphorus, and hydrogen atoms, respectively.

The $3 \times 3 \times 1$ 4H-SiC (0001) supercell consists of four bilayers of SiC with a vacuum space of 10 Å in dimension. The carbon dangling bonds at the bottom layer are terminated by hydrogen atoms and the bottom three layers are fixed to simulate the infinitely large bulk solid. A converged $3 \times 3 \times 1$ Monkhorst–Pack k-point mesh[31] is used during the geometry optimizations of various surface models. On the SiC (0001) surface, P adatoms are initially placed on four high-symmetric adsorption sites as shown in Fig. 1. The adsorption energy per P adatom is calculated as follows:

$$E^{\mathrm{P}}_{\mathrm{ads}} = (N_{\mathrm{P}} \cdot E_{\mathrm{P}} + E_{\mathrm{slab}} - E_{\mathrm{P/slab}})/N_{\mathrm{P}}, \tag{1}$$

where N_{P} is the number of P atoms adsorbed on the 4H-SiC (0001) surface, and E_{P}, E_{slab}, and $E_{\mathrm{P/slab}}$ refer to the total energies of the isolated P atom, and the surfaces with and without the P adatoms, respectively.

The stability of each structure is assessed by calculating the Gibbs free energy of formation ΔG_{form} in the grand canonical ensemble

$$\Delta G_{\mathrm{form}} = E_{\mathrm{P/slab}} - E_{\mathrm{slab}} - N_{\mathrm{P}}\mu_{\mathrm{P}}, \tag{2}$$

where μ_{P} is the chemical potential of P atom. Combining Eqs. (1) and (2), one can obtain

$$\Delta G_{\mathrm{form}} = -N_{\mathrm{P}}E^{\mathrm{P}}_{\mathrm{ads}} - N_{\mathrm{P}}\Delta\mu_{\mathrm{P}}, \tag{3}$$

with $\Delta\mu_{\mathrm{P}} = \mu_{\mathrm{P}} - E_{\mathrm{P}}$.

3. Results and discussion

We start our analysis by studying P atom adsorption on the 4H-SiC (0001) surface. For a single P atom adsorption, corresponding to 1/9 monolayer (ML) coverage in our supercell model, only the H3 and T4 binding configurations are stable. According to the calculated result, the H3 site is more favorable since its adsorption energy is 0.19 eV higher than that of the configuration with a P atom at the T4 site. For the 2/9 ML coverage surface, five possible stable configurations are obtained after optimizing 37 initial structures. Unlike the nitrogen adsorption on 4H-SiC,[18] the most energetically favorable configuration is the one with two P atoms at different T4 sites rather than different H3 sites. It is interesting that the most stable location for P atoms shifts from the H3 site to T4 site. This might be attributed to the strong interaction between two P atoms which makes the P adatoms deviate from the H3 sites. When three P atoms are deposited on the supercell of 4H-SiC surface (i.e., 1/3 ML coverage), these P atoms still prefer separated T4 sites. It is also found that this coverage has a $(\sqrt{3} \times \sqrt{3})$ R30° pattern. Above 4/9 ML coverage, the P adatoms rearrange their bonding on the surface and form P2 dimer or P3 ring. As the coverage reaches 1 ML, three P3 rings appear symmetrically on the SiC surface. In this configuration, each P3 ring is located at the T4 site with three P–P bonds of about 2.215 Å.

The dependence of the adsorption energy per P atom on the phosphorus coverage is illustrated in Fig. 2. The positive adsorption energies suggest that the reactions between the P atoms and the surface atoms are exothermic. For the 1/9 ML configuration, the corresponding adsorption energy per P atom is 2.68 eV. With the increase of the coverage, the adsorption

energy reaches maximum at 1/3 ML coverage, and then significantly decreases from 2.79 eV at 1/3 ML to 1.80 eV at 2/3 ML coverage. When the coverage exceeds 2/3 ML, the adsorption energy becomes relatively stable.

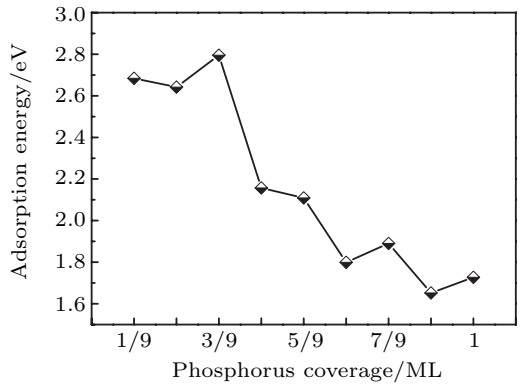


Fig. 2. The Gibbs free energy of formation as a function of phosphorus coverage.

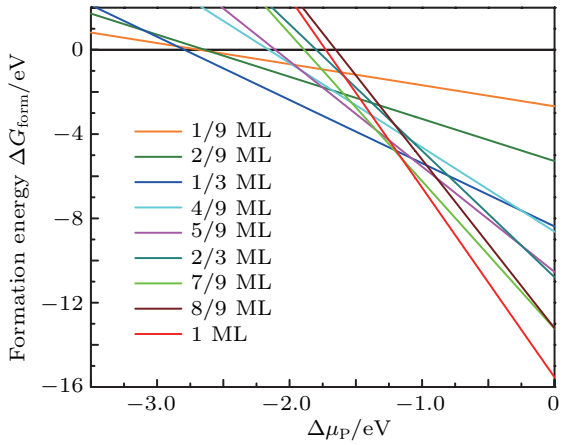


Fig. 3. (color online) Adsorption energy per phosphorus adatom as a function of phosphorus chemical potential.

To determine the stability of various P/slab configurations, we plot the Gibbs free energy of formation as a function of phosphorus chemical potential using Eq. (3). This surface diagram describes the most stable structure at different chemical potentials related to a realistic gas environment. The formation energy of bare SiC surface ($\Delta G_{\rm form} = 0$) is marked by the black horizontal line as a reference. When $\Delta\mu_{\rm P} < -2.79$ eV, the bare 4H-SiC (0001) surface is the most stable structure. As the phosphorus chemical potential increases from -2.79 eV to -1.20 eV, the 1/3 ML configuration becomes most energetically favorable. When $\Delta\mu_{\rm P} > -1.20$ eV, the 1 ML configuration is stable. Considering the fact that the P atom is difficult to diffuse into the SiC surface, only the 1/3 ML configuration may be observed as a stable structure. That the 1/3 ML adsorption configuration is energetically favorable may be simply explained as follows. On the 4H-SiC surface, each surface Si atom has one unsaturated electron (i.e., a dangling bond). This gives rise to the surface with threefold symmetry adsorption sites, which are considered more favorable than the others. One P atom with three valence electrons and two lone-pair electrons is able to form a covalent bond with each of the three surface Si atoms. Thus, the surface dangling bonds could be fully saturated at 1/3 ML coverage. This picture can be further confirmed by the analysis of electron densities.

Figure 4 depicts the electron densities of the most stable P/4H-SiC (0001) configurations, in which the green and the blue parts represent the electron accumulation and depletion regions, respectively. Clearly, electrons transfer from the surface Si atoms to the P adatoms, which indicates the formation of P–Si bonds. At the 1/3 ML coverage, three P atoms can form nine P–Si bonds; thus the 4H-SiC (0001) surface can be completely saturated through post-oxidation annealing in $POCl_3$.

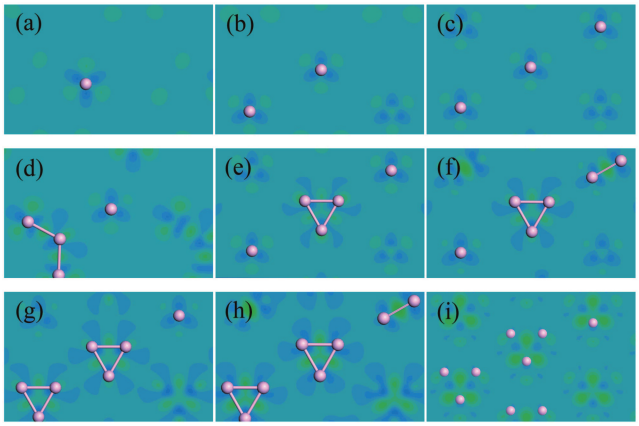


Fig. 4. (color online) Different electron densities of the stable configurations for the coverages of (a) 1/9 ML, (b) 2/9 ML, (c) 1/3 ML, (d) 4/9 ML, (e) 5/9 ML, (f) 2/3 ML, (g) 7/9 ML, (h) 8/9 ML, (i) 1 ML. The violet spheres denote phosphorus atoms.

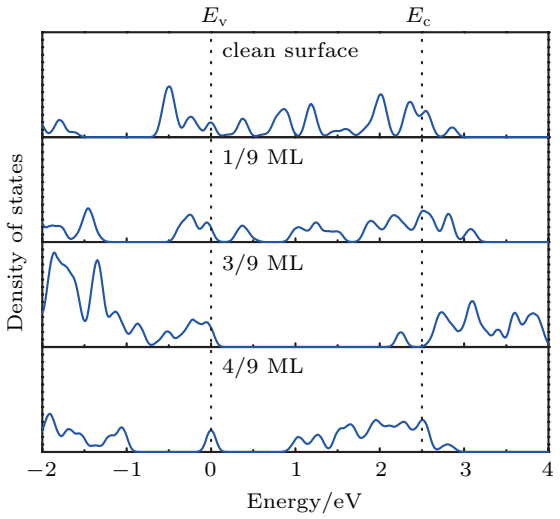


Fig. 5. (color online) Total densities of states for the clean surface and surfaces with 1/9 ML, 1/3 ML, and 4/9 ML phosphorus coverages.

To further elucidate the phosphorus passivation effects on the density of interface traps, we present the electron densities of states (DOS) for the clean surface, 1/9 ML, 1/3 ML, and 4/9 ML coverage as shown in Fig. 5. For the clean surface, the calculated DOS near the conduction band is high enough in the

band gap, which agrees with the experimental observation.[14] Comparing the DOS for different coverage, we find that the DOS near the conduction band decreases with the coverage increasing from 1/9 to 1/3 ML, and then increases again when the coverage is higher than 1/3 ML. Here we are most interested in the 1/3 ML configuration since it is most energetically favorable in a reasonable physical condition. At 1/3 ML, the DOS inside the band gap is almost completely eliminated. In other words, the P adatoms play an effective passivation role for 4H-SiC (0001) Si dangling bonds.

4. Conclusion

We investigate adsorption behaviors of P atoms on 4H-SiC (0001) and effects of P passivation on surface Si dangling bonds by using density functional theory methods. The surface diagram result indicates that the 1/3 ML configuration is most energetically favorable (i.e., a reasonable phosphorus concentration). At this coverage, the density of surface states within the band gap of bare surface is found to be decreased. It also shows that P passivation removes states from the conduction band gap. This is similar to the previous experimental observation[22,26] even though a complicated oxide during P passivation is not theoretically considered. Therefore, the physical mechanisms of P passivation of the bare SiC surface may also play a role during P passivation of the SiO_2/SiC interface. The presence of P atoms at the SiO_2/SiC interface region can effectively eliminate Si dangling bonds and decrease the interface state density.

References

[1] Ruff M, Mitlehner H and Helbig R 1994 *IEEE Trans. Electron Devices* **41** 1040
[2] Nakamura D, Gunjishima I, Yamaguchi S, Ito T, Okamoto A, Kondo H, Onda S and Takatori K 2004 *Nature* **430** 1009
[3] Melinon P, Masenelli B, Tournus F and Perez A 2007 *Nat. Mater.* **6** 479
[4] Presser V and Nickel K G 2008 *Crit. Rev. Solid State Mater. Sci.* **33** 1
[5] Cooper J A 1997 *Phys. Status Solidi A* **162** 305
[6] Ventra M D and Pantelides S T 1999 *Phys. Rev. Lett.* **83** 1624
[7] Afanasév V V, Bassler M, Pensl G and Schultz M 1997 *Phys. Status Solidi A* **162** 321
[8] Afanasév V V and Stesmans A 1997 *Phys. Rev. Lett.* **78** 2437
[9] Knaup J M, Deák P, Frauenheim T, Gali A, Hajnal Z and Choyke W J 2005 *Phys. Rev. B* **71** 235321
[10] Zhu Q, Huang L, Li W, Li S and Wang D 2011 *Appl. Phys. Lett.* **99** 082102
[11] Jia Y, Lv H, Niu Y, Li L, Song Q, Tang X, Li C, Zhao Y, Xiao L, Wang L, Tang G, Zhang Y and Zhang Y 2016 *Phys. B* **25** 097101
[12] Li H, Dimitrijev S, Harrison H B and Sweatman D 1997 *Appl. Phys. Lett.* **70** 2028
[13] Dhar S, Wang S, Williams J R, Pantelides S T and Feldman L C 2005 *MRS Bull.* **30** 288
[14] Chung G Y, Tin C C, Williams J R, McDonald K, Di Ventra M, Pantelides S T, Feldman L C and Weller R A 2000 *Appl. Phys. Lett.* **76** 1713
[15] Yano H, Hirao T, Kimoto T and Matsunami H 2001 *Appl. Phys. Lett.* **78** 374
[16] Wang S, Dhar S, Wang S, Ahyi A C, Franceschetti A, Williams J R, Feldman L C and Pantelides S T 2007 *Phys. Rev. Lett.* **98** 026101
[17] Deák P, Knaup J M, Hornos T, Thill C, Gali A and Frauenheim T 2007 *J. Phys. D: Appl. Phys.* **40** 6242
[18] Ashman C R, Först C J, Schwarz K and Blöchl P E 2004 *Phys. Rev. B* **69** 075309
[19] Pennington G and Ashman C R 2007 *Appl. Phys. Lett.* **91** 072106
[20] Ashman C R and Pennington G 2008 *Surf. Sci.* **602** 3617
[21] Ashman C R and Pennington G 2009 *Phys. Rev. B* **80** 085318
[22] Okamoto D, Yano H, Hatayama T and Fuyuki T 2010 *Appl. Phys. Lett.* **96** 203508
[23] Okamoto D, Yano H, Hirata K, Hatayama T and Fuyuki T 2010 *IEEE Electron Device Lett.* **31** 710
[24] Okamoto D, Yano H, Kotake S, Hirata K, Hatayama T and Fuyuki T, 2010 *MRS Symp. Proc.* 1246-B06-06
[25] Okamoto D, Yano H, Hatayama T and Fuyuki T 2012 *Materials Science Forum* **717–720** 733
[26] Okamoto D, Yano H, Kotake S, Hirata K, Hatayama T and Fuyuki T 2011 *Materials Science Forum* **679–680** 338
[27] Cantin J L, Von Bardeleben H J, Shishkin Y, Ke Y, Devaty R P and Choyke W J 2004 *Phys. Rev. Lett.* **92** 015502
[28] Lenahan P M and Conley J F 1998 *J. Vac. Sci. Technol. B* **16** 2134
[29] Perdew J P and Wang Y 1992 *Phys. Rev. B* **45** 13244
[30] Vanderbilt D 1990 *Phys. Rev. B* **41** 7892
[31] Monkhorst H J and Pack J D 1976 *Phys. Rev. B* **13** 5188